Dalton Transactions

Bridging the opposite chemistries of tantalum and tungsten polyoxometalates

Journal:	*Dalton Transactions*
Manuscript ID:	DT-ART-06-2015-002290
Article Type:	Paper
Date Submitted by the Author:	17-Jun-2015
Complete List of Authors:	Molina, Pedro; Oregon State University, Chemistry Sures, Dylan; Oregon State University, Chemistry Miro, Pere; University of Minnesota, Department of Chemistry Zakharov, Lev; Oregon State University, Department of Chemistry Nyman, May; Oregon State University,

Dalton Transactions

ARTICLE

Bridging the opposite chemistries of tantalum and tungsten polyoxometalates

Received 00th January 20xx,
Accepted 00th January 20xx

DOI: 10.1039/x0xx00000x

www.rsc.org/

P.I. Molina,[a] D. J. Sures,[a] P. Miró,[b] L. N. Zakharov[a] and M. Nyman[a]

The disparate solubility, redox activity, and pH stability of the group V and group VI polyoxometalates (POMs) confer very different functionality on these species, and tailoring cluster properties by varying the ratio of group V to group VI metals poses both an opportunity and a synthetic challenge. A classic series of studies reported over 40 years ago provided some insight into W/Nb POMs, from which researchers have built on to date. However, the analogous W/Ta series has never been addressed in a systematic manner. Three members of this W/Ta series are presented here, synthesized from simple oxo- and peroxocoltanate precursors. $[Ta_3W_3O_{19}]^{5-}$ displays the Lindqvist-type structure, while $[TaW_9O_{32}]^{5-}$ and $[Ta_2W_8O_{32}]^{6-}$ are isostructural with decatungstate ($[W_{10}O_{32}]^{4-}$). Additionally, the use of peroxoniobate instead of hexaniobate as the starting material drives the formation of the decatungstate-type structure $[NbW_9O_{32}]^{5-}$ instead of the Lindqvist ion that was established to be the foundational cluster geometry in prior work. The electronic structure of the Nb/Ta substituted decatungstates is directly related to the degree of substitution inasmuch as the HOMO-LUMO energy gap (E_{gap}) slightly increases as more Nb/Ta atoms are incorporated into the structure. The poor mixing of the d-orbitals of Nb/Ta and W is responsible for the observed trends in the UV spectra and cyclic voltammetry. Moreover, the stability of the molecular frameworks in the gas phase is also related to the extent of substitution as revealed by electrospray mass-spectrometry (ESI-MS).

Introduction

Group V (V, Nb and Ta) and group VI (Mo and W) are the main polyoxometalate (POM) forming metals.[1] The group V and group VI POMs share a number of cluster geometries based on the assembly of distorted metal-oxo polyhedra, and the presence of the inert '*yl*' oxygen at their outer surface.[2] However, the aqueous stability and behaviour of POMs varies remarkably as a function of elemental composition. Group VI POMs (W and Mo) and polyvanadates are generally stable under acidic and neutral conditions while polycoltanates[3] (Nb and Ta) are stable in base. Moreover, the aqueous solubility trends of their alkali metal salts have been shown to be opposite as the Cs^+ salts of polycoltanates are extremely soluble[4] while their Li^+ salts are rather insoluble[5] and the exact reverse applies to group VI POMs. These contrasting solubilities are surely related to their difference in charge density and ion-association behaviour, yet the underlying causes of this phenomenon are not fully understood. This difference also plays a major role in their disparate electrochemical behaviour as densely charged polycoltanates are redox inert while group VI POMs, and especially polytungstates, display a rich and robust electrochemical activity.[6] In general, aqueous ion-association plays a crucial role in the control of many geochemical, biochemical, and synthetic processes. Specific to this study, fundamental insights into these properties would help to elucidate their effect in a number of relevant POM functionalities such as catalysis,[7-8] interaction with biomolecules[9] and assembly into framework materials,[10] to name just a few. Moreover, given the discrete and monodisperse nature of POMs, they can serve as model systems for computational and experimental understanding of the interrelated phenomena of ion-association, electron transfer, and acid-base chemistry.

A rational strategy to address those questions requires the synthesis of mixed metal Nb/Ta polytungstates showing a stepwise range of elemental ratios. Recent work in synthesizing W/Nb or W/Ta POMs has entailed the reaction of lacunary polytungstates with the Lindqvist ion $[M_6O_{19}]^{8-}$ (M = Nb, Ta) in water/H_2O_2 mixtures. The presence of peroxide in these reaction systems is paramount as these ligands temporarily prevent the precipitation of Nb/Ta oxyhydroxide in the pH range at which polytungstates are stable. This approach has yielded several polyanions displaying a non-systematic range of oxo-Nb[11-14] and -Ta[15, 16] cores stabilized by lacunary tungstate fragments; that is, a similar outcome to the extensive syntheses of transition metal

[a] Department of Chemistry, Oregon State University, 107 Gilbert Hall, Corvallis, OR, 97331-4003, USA. Email: May.Nyman@oregonstate.edu
[b] Department of Physics and Earth Sciences, Theoretical Physics - Theoretical Material Science, Jacobs University, Bremen, Germany.
Electronic Supplementary Information (ESI) available: Experimental procedures, computational details, crystallography, BVS, ESI-MS, CV, UV-Vis, TGA, SEM, EDX, FTIR and additional computational plots and tables. See DOI: 10.1039/x0xx00000x

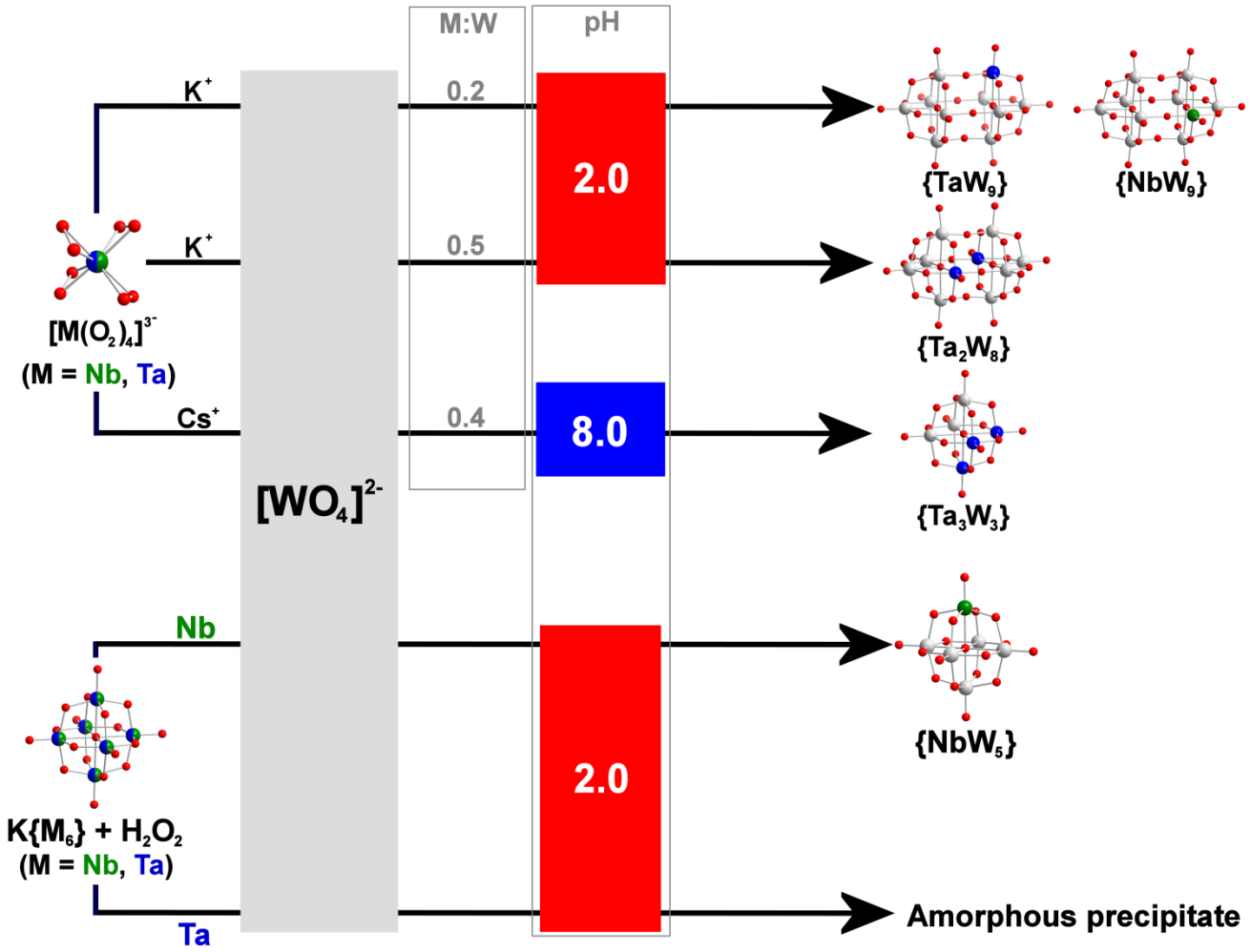

Scheme 1. Key parameters in the synthesis of $Cs_4Na[Ta_3W_3O_{19}]$ ($CsNa\{\mathbf{Ta_3W_3}\}$), $Cs_5[NbW_9O_{32}]$ ($Cs\{\mathbf{NbW_9}\}$), $Cs_5[TaW_9O_{32}]$ ($Cs\{\mathbf{TaW_9}\}$) and $Cs_6[Ta_2W_8O_{32}]$($Cs\{\mathbf{Ta_2W_8}\}$).

substituted polyoxotungstates. A more rational approach was implemented almost forty years ago by Dababbi and co-workers to produce a series of $[Nb_xW_{6-x}O_{19}]^{(2+x)-}$ (x = 1-4) isopolyanions from reactions of tungstate and hexaniobate in water/H_2O_2.[17] A subsequent report focused on the aqueous electrochemistry of these clusters to reveal that their ability to be reduced diminished rapidly with increasing Nb content.[18] This first study was followed by reports on 1) crystallographic analysis of the first two W-rich member of the series,[19-22] 2) alternative syntheses for spectroscopic analysis in non-aqueous solvents,[20, 23, 24] and 3) $[Nb_xW_{6-x}O_{19}]^{(2+x)-}$ as inorganic ligands in the assembly of hybrid complexes[25-27] or dimers[22, 28] on account of the increased basicity of the oxygen atoms bound to Nb centres. The analogous Ta/W series has never been systematically investigated inasmuch as only the first member of the series,[23] and its Ta-O-Ta linked dimer,[29] have been synthesized in non-aqueous solvents. Therefore, it becomes apparent that having access to a mixed metal Nb/W and Ta/W cluster series would provide an excellent opportunity to determine the composition at which the transition from polytungstate to polycoltanate character occurs in terms of ion-pairing, redox activity and solubility of the alkali metal salts.

As we advance the exploration of the synthetic parameter space of polycoltanates,[2, 30] and their ion-association in solution,[31, 32] we herein present one Nb/W and three Ta/W polyanions (Scheme 1): $[Ta_3W_3O_{19}]^{5-}$, a Lindqvist-type polyanion isolated as the mixed Cs^+/Na^+ salt ($Cs_4Na[Ta_3W_3O_{19}]\cdot 6H_2O$, $CsNa\{\mathbf{Ta_3W_3}\}$), and $[NbW_9O_{32}]^{5-}$, $[TaW_9O_{32}]^{5-}$ and $[Ta_2W_8O_{32}]^{6-}$, clusters isostructural with decatungstate and isolated as pure Cs^+ salts ($Cs_5[NbW_9O_{32}]\cdot 7H_2O$, $Cs\{\mathbf{NbW_9}\}$; $Cs_5[TaW_9O_{32}]\cdot 6.5H_2O$, $Cs\{\mathbf{TaW_9}\}$; $Cs_6[Ta_2W_8O_{32}]\cdot 6H_2O$, $Cs\{\mathbf{Ta_2W_8}\}$). These studies also contribute to our understanding of the relationships in polyanions between initial synthetic conditions and final isolated structure and between the Nb/Ta to W elemental ratio and the electronic properties.

Results and discussion

Synthesis

Nb and Ta peroxide complexes have been employed as precursors for framework oxide materials during the past few decades.[33] Furthermore, these complexes have been used as precursors to synthesize $[Ta_6O_{19}]^{8-}$ [30, 32] using a softer and more controllable approach to the original ones based on Ta_2O_5/alkali digestions.[34] Here we extend the use of peroxocoltanate $[M(O_2)_4]^{3-}$ (M = Nb, Ta) as the starting material for the synthesis of Nb/Ta polytungstates to exert a greater control in the synthesis by avoiding use of excess peroxide. Three Ta/W (**{Ta_3W_3}**, **{TaW_9}** and **{Ta_2W_8}**) and one Nb/W (**{NbW_9}**) polyanions were isolated from acidified mixtures of these peroxometalates, Na_2WO_4, HCl and water/H_2O_2 under strict pH control.

{Ta_3W_3} was isolated from refluxed, alkaline (pH = 8.0) reaction mixtures as colourless crystals. The presence of Na^+ in the reaction was required for crystallization, as reactions in which Cs_2WO_4 replaced Na_2WO_4 failed to yield any crystalline material.

Isostructural **{NbW_9}**, **{TaW_9}** and **{Ta_2W_8}**, were isolated from reaction mixtures similar to that for **{Ta_3W_3}** albeit at lower values of pH (2.0). Acidic suspensions of $K_3[M(O_2)_4]$ (M = Nb, Ta) and Na_2WO_4 would turn creamy yellow upon heating and the isolated clear, bright yellow, solution would yield Cs**{NbW_9}** or Cs**{TaW_9}** as thick yellow precipitates upon the addition of excess Cs^+. Our attempts to introduce more Ta centres in the decatungstate structure resulted in the isolation of Cs**{Ta_2W_8}**, from reaction mixtures of higher Ta:W ratio. However, an equivalent strategy to prepare $[Nb_2W_8O_{32}]^{6-}$ was not met by successful, and the Lindqvist ion $[Nb_2W_4O_{19}]^{4-}$ was obtained instead.

The nuclearity of the Nb/Ta reagent has a direct impact in the structure of the isolated reaction product. Dabbabi *et al.* isolated Lindqvist-type $Cs_3[NbW_5O_{19}]$ using $K_8[Nb_6O_{19}]$ as a starting material[17] while we isolated the substituted decatungstates **{NbW_9}**, **{TaW_9}** and **{Ta_2W_8}** as pure Cs^+ salts from equivalent reaction systems in which $K_3[M(O_2)_4]$ (M = Nb, Ta) replaced $K_8[Nb_6O_{19}]$. Intriguingly, reactions of $[Ta_6O_{19}]^{8-}$ or $[Ta(O_2)_4]^{3-}$ under equivalent conditions failed to yield $[TaW_5O_{19}]^{3-}$, a cluster that has been isolated solely from non-aqueous reaction systems.[23] Control reactions in which neither Nb nor Ta was present in the reaction mixture produced crystals of dodecatungsate, $Cs_6[H_2W_{12}O_{40}]\cdot nH_2O$, as identified by At% ratio (EDX) and unit cell determination.[35] Thus, $[TaW_5O_{19}]^{3-}$ does not seem to form in water under similar conditions in which $\{NbW_5\}$ forms, an observation which highlights the subtle differences, despite their nearly identical size, between the aqueous chemistries of Nb and Ta. In fact, and based on recent reports, in these acidic conditions Ta emulates the transition metals outside of the metal-oxo wall.[15, 16] This is probably due to the higher reactivity of its O/OH/H_2O ligands which necessitates stabilization inside a tungstate 'shell'.

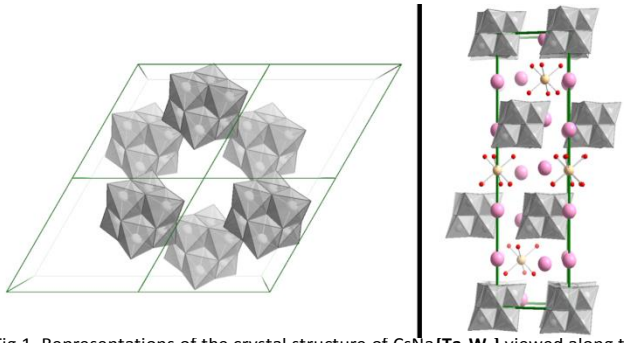

Fig 1. Representations of the crystal structure of CsNa**{Ta_3W_3}** viewed along the *c* (left) and *b* (right) crystallographic axes. Colour code: Colour code: $\{MO_6\}$ (M = W^{VI}, Ta^V), grey polyhedra/wireframe; Cs^+, pink spheres; Na^+, teal spheres; O, red spheres.

Structures

CsNa**{Ta_3W_3}** crystallises in the trigonal crystal system (Table S1) and there is only one symmetrically inpendent metal position in the cluster unit**.** Hence, Ta and W are disordered over the six metal positions of the cluster and the occupancy of each metal site matches the Ta/W ratio of the whole cluster. A ratio close to 0.5:0.5 for Ta/W is found in the free refinements of those crystallographic positions and this ratio is supported by the At% ratio (EDX) and the crystallographic determination of the required number of countercations to balance the charge of the compound. The **{Ta_3W_3}** clusters in the crystal structure arrange on layers stacked along the *c* axis and chains of four Cs^+ and one $[Na(H_2O)_6]^+$ align on axes perpendicular to those layers as shown in Fig 1 and Fig S2-S3.

The values of bond distances between the metal centres and the three inequivalent types of oxo ligands (Fig S7) in **{Ta_3W_3}** fall in the expected range for a Ta/W mixed metal cluster. The bond distance between the mixed-metal site and the terminal oxo ligands (O_t) of **{Ta_3W_3}** (1.769(10) Å) is slightly closer to the reported values for $[Ta_6O_{19}]^{8-}$ ({Ta_6}, 1.811(25) Å)[36] than to the ones for $[W_6O_{19}]^{2-}$ ({W_6}, 1.689(6) Å).[37] This trend is repeated in the M-O_b distances, as the average value in **{Ta_3W_3}** (1.954(17) Å) is closer to the one in hexatantalate (1.975(16) Å) than in hexatungstate (1.924(3) Å), and also in the M-O_c distances, *i.e.* 2.361(1) Å in **{Ta_3W_3}**, 2.353(32) Å in {Ta_6} and 2.331(4) Å in {W_6}. The inclusion of Ta in the structure of {W_6} therefore results in the lengthening of bond distances, on account of two factors: the lower charge of Ta^V compared to W^{VI} and the presence of two different metals in the same structure, which typically distorts the molecular framework. The average of the values for the angles described by two metal centres and each of the O_b atoms are similar in **{Ta_3W_3}** (117(1)°), $[Ta_6O_{19}]^{8-}$ (115(1)°) and $[W_6O_{19}]^{2-}$ (118(1)°).

Bond-Valence Summation (BVS) (Table S8) analysis indicates that none of the oxo ligands in **{Ta_3W_3}** are protonated, which also agrees with the direct localization of all the alkali counterions required to balance the charge of the crystal structure, and that the unique crystallographically independent metal site is occupied by W and Ta (Table S12). The disorder in the metal positions in the crystal structure

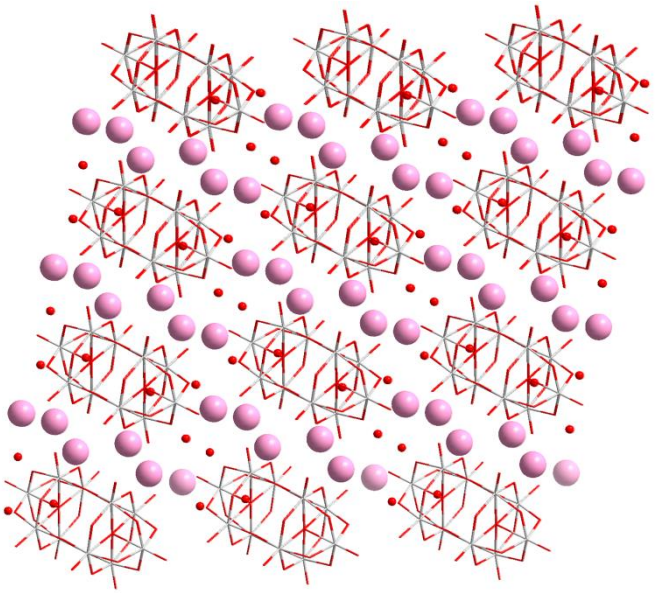

Fig 2. Crystal structure of Cs**{Ta_2W_8}** viewed along the crystallographic b axis Colour code: {MO_6} (M = W, Ta), grey-red wireframe; Cs^+, pink spheres; O, red spheres.

does not allow the BVS analysis to support any particular assignment of the oxidation state of the metal centres. However, it is safe to assume that neither Ta nor W are reduced owing to the absence of a reducing agent from the reaction mixtures and the yellow-white coloration of the products, typical of fully oxidised polytantalates/polytungstates which is also reflected in the absence of an absorption band in the visible region of the UV-vis spectrum (Fig S17) as opposed to the typical blue colour of reduced Nb/Ta/W.

{Ta_3W_3} is assigned as the *fac* isomer, [*fac*-$Ta_3W_3O_{19}]^{5-}$, on the basis of FTIR spectroscopy. The two bands at 528 and 567 cm^{-1} (Fig S26), ascribed to the stretching modes of the M-O_c bonds, are equivalent to the bands at 565 and 522 cm^{-1} found in [*fac*-$Nb_3W_3O_{19}$].[38]

Cs**{NbW_9}**, Cs**{TaW_9}** and Cs**{Ta_2W_8}** crystallise in the triclinic system under similar unit cell dimensions (Table S1).The Nb/W and Ta/W ratio in polyanions **{NbW_9}**, **{TaW_9}** and **{Ta_2W_8}** are established on the basis of the At% ratio (EDX) and charge balance considerations. These three clusters are isostructural to decantugstate {W_{10}}[39] and [$ReW_9O_{32}]^{5-}$.[40]

The information on bond distances and angles available from the crystallographic structures is limited due to the disorder of the metal positions. An inspection of the average values of bond distances reveals that they are close to the typical values for {W_{10}}.[41] The average M=O_t (Fig S7) bond distances are 1.733(10) Å, 1.722(6) Å and 1.731(28) Å for **{NbW_9}**, **{TaW_9}** and **{Ta_2W_8}**, respectively; values that compare well with the value of 1.74(3) Å in {W_{10}}. Similarly, the values of the average M-O_c (μ_5-O ligand) bond distances are 2.340(33) Å in **{NbW_9}**, 2.322(25) Å in **{TaW_9}** and 2.330(55) Å in **{Ta_2W_8}**, values close to the equivalent parameter in {W_{10}}, 2.30(4) Å. Finally, an analogous comparison between average distances of the metal/μ_2-O bonds yields similar results: 1.943(25) Å in **{NbW_9}**, 1.928(25) Å in **{TaW_9}** and 1.934(29) Å in **{Ta_2W_8}** *vs.* the value of 1.93(4) Å.

BVS analysis of **{NbW_9}**, **{TaW_9}** and **{Ta_2W_8}** confirm that the oxo ligands are not protonated and that the metal sites show mixed metal occupancy. Similarly as for **{Ta_3W_3}**, the oxidation of the state of the metal centres cannot be obtained from the BVS analysis (Tables S13-S15) yet it may be established from spectroscopic, *i.e.* the absence of absorption bands in the visible region which may be caused by reduced metal centres (Fig S17) and synthetic considerations (absence of a reducing agent).

The crystal structures of Cs**{NbW_9}** Cs**{TaW_9}** **and** Cs**{Ta_2W_8}** are centrosymmetrical and there are five symmetrically independent positions in the cluster units of which the four equatorial ones (M2, Fig S7) are occupied by Nb/W and the apical position (M1, Fig S7) is fully occupied by W. This differential assignment of the equatorial and apical positions of the structure stems from the significant disparity in number of electrons of Nb and W. Free refinement of the W occupation factors on the M1/M2 positions yield a value very close to 1 for M1 and considerably lower for M2. The occupation factors at these four M2 positions obtained from a refinement treating such positions as occupied by Nb/W are 0.88/0.12, 0.89/0.11, 0.88/0.12 and 0.88/0.18. The eventual refinement of Cs**{NbW_9}** was performed by fixing the M1 apical position as fully occupied by W and the four M2 equatorial positions as Nb/W at a 0.125/0.875 ratio to correctly balance the charge of the compound. Finally, this assignment of the metal positions in the Cs**{NbW_9}** structure is supported by theory as substitution of Nb/Ta at the apical position is energetically disfavoured as it will be discussed in more detail below. In the case of **{TaW_9}** and **{Ta_2W_8}**, the content of the electronic shells of Ta^V and W^{VI} is identical ($[Xe]4f^{14}$) and therefore X-ray diffraction cannot assign any of the metal positions as occupied solely by W or Ta. Hence, the final refinements of these two structures were performed in a similar fashion as for Cs**{NbW_9}** and this refinement strategy is also supported by calculation (see below).

The crystal structures of the three compounds, **{NbW_9}**, **{TaW_9}** and **{Ta_2W_8}**, are fairly similar inasmuch as the main differences relate to the occupancy and disorder of the countercation sites and solvent molecules. A representation of the crystal structure of **{Ta_2W_8}** is shown in Fig 2 as an example for the structures of the three compounds while Fig S4 shows two more simplified representations of this structure highlighting the coordination of the Cs^+ countercations by the solvent water molecules and the position of those countercations in the unit cell. Representations of the crystal structure of **{NbW_9}** are shown in Fig S5-S6.

ESI-MS

Electrospray-ionisation mass-spectrometry (ESI-MS) was employed to explore the stability of the four compounds in solution and in the gas phase. Spectra of CsNa**{Ta_3W_3}**, Cs**{NbW_9}**, Cs**{TaW_9}**, Cs**{Ta_2W_8}** and $K_4[W_{10}O_{32}]$ (K{W_{10}}) were obtained from solution in H_2O/CH_3CN mixtures. The regions of

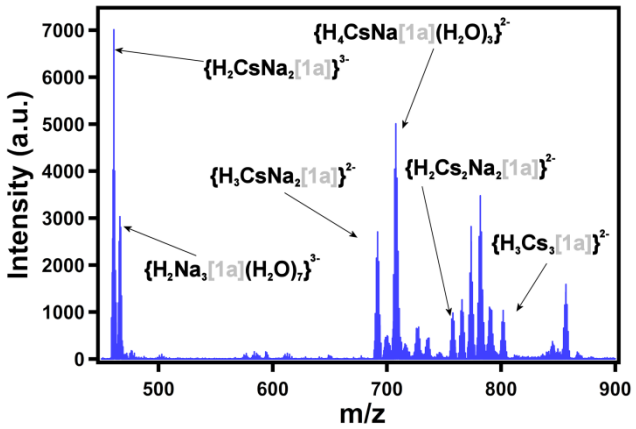

Fig 3. ESI-MS of Cs{Ta_3W_3}. Code: [1a], $[Ta_2W_3O_{18}]^{8-}$

interest of these spectra, along with labelled peak envelopes, are shown in Fig 3-4 while Table S16 summarizes the assignments for those peak envelopes.

Our results suggest that the stability in the gas phase of the clusters is related to the degree of substitution of the polytungstate framework. Intact $\{W_{10}\}$, **{NbW$_9$}** and **{TaW$_9$}** are observed in their corresponding spectra while in the case of **{Ta$_3$W$_3$}** and **{Ta$_2$W$_8$}** only lacunary fragments can be detected. All fragments and intact ions are detected as species hydrated and associated to cations, adventitious or present in the compound, to a different degree. The monolacunary fragment $[Ta_2W_3O_{18}]^{8-}$, in which a Ta^{V}=O unit is lost from the parent ion is the dominant specie in the gas phase of the spectrum of **{Ta$_3$W$_3$}**. A related lacunary fragment of the related polytungstate $\{W_5\}$(=$[W_5O_{16}]^{2-}$) has been previously detected in ESI-MS studies of $[W_6O_{19}]^{2-}$.[42] Monolacunary fragments were not observed in the ESI-MS studies of Lindqvist type polycoltanates at high pH.[43] An analogous lacunary fragment $\{CoW_4\}$(=$[CoW_4O_{14}]^{2-}$) was observed in the mass spectrum of dimeric $[\{CoW_5O_{18}H\}_2]^{6-}$.[44] The spectrum of **{Ta$_2$W$_8$}** also yields a monolacunary fragment, $[Ta_2W_7O_{31}]^{10-}$. Interestingly, this fragment is generated by the loss of a W^{VI}=Ot unit as opposed to the case of **{Ta$_3$W$_3$}**, in which the lost unit is Ta^{V}=O_t. Both spectra of Cs**{NbW$_9$}** and Cs**{TaW$_9$}** show the intact parent ions, **{NbW$_9$}** and **{TaW$_9$}**, and monolacunary fragments $[NbW_8O_{31}]^{9-}$ and $[TaW_8O_{31}]^{9-}$ produced by the loss of a W^{VI}=O_t unit. This is the first report on the gas phase behaviour, *via* ESI-MS analysis, of $\{W_{10}\}$ and substituted derivatives, benchmarking their stability along with the computational studies discussed later.

UV-Vis spectroscopy / Electrochemistry

The electrochemical behaviour of polytungstates and polycoltanates is significantly different. Polytungstates can be reversibly reduced to a varying extent under a range of

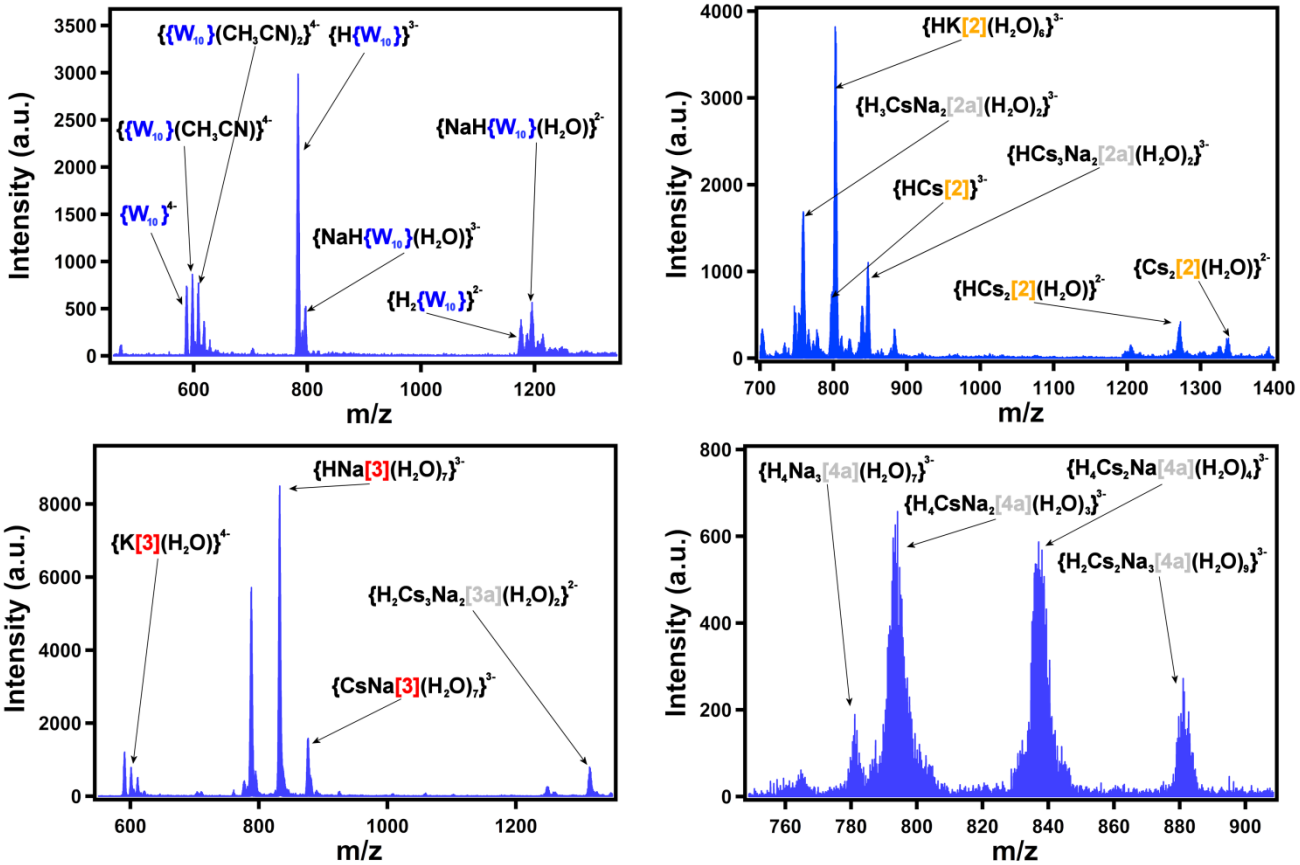

Fig 4. ESI-MS spectra of $K_4[W_{10}O_{32}]$ ($\{W_{10}\}$) (top left), **{NbW$_9$}** (top right), **{TaW$_9$}** (bottom left) and **{Ta$_2$W$_8$}** (bottom right). Codes: [2] = $[NbW_9O_{32}]^{5-}$, [2a] = $[NbW_8O_{31}]^{9-}$, [3]= $[TaW_9O_{32}]^{5-}$, [3a] = $[TaW_8O_{31}]^{9-}$, [4a] = $[Ta_2W_8O_{31}]^{10-}$.

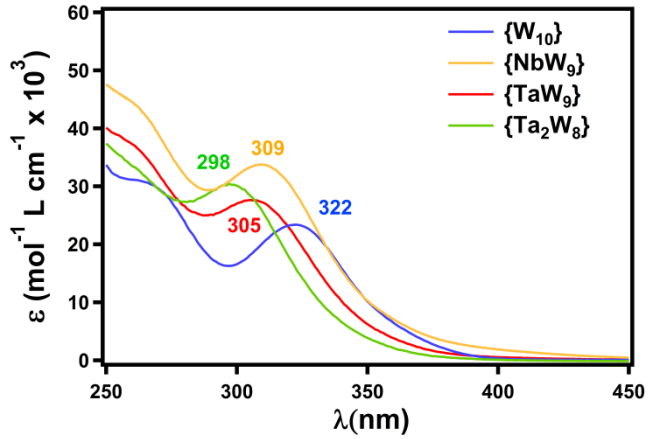

Fig 5. UV-vis spectra of aqueous solutions of $K_4[W_{10}O_{32}]$ ($\{W_{10}\}$, blue), **{NbW$_9$}** (orange), **{TaW$_9$}** (red) and **{Ta$_2$W$_8$}** (green). The wavelength values of the absorption bands assigned to the linear M-O-M bonds O→M charge transfers are highlighted.

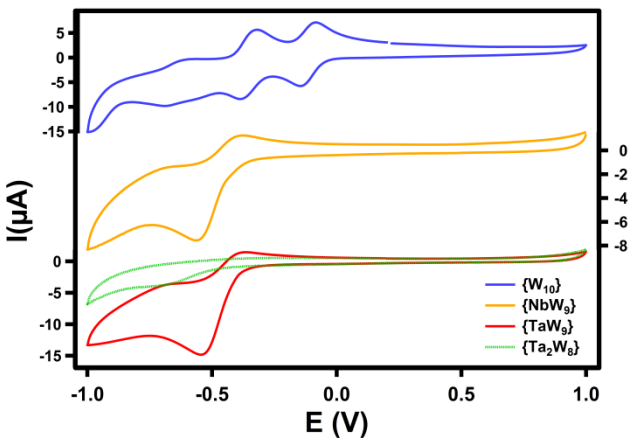

Fig 6. Cyclic voltammograms of $K_4[W_{10}O_{32}]$ ($\{W_{10}\}$, blue), **{NbW$_9$}** (orange), **{TaW$_9$}** (red) and **{Ta$_2$W$_8$}** (green) in aqueous 0.2 M LiCl. The scan speed was 100 mV s^{-1}. The working, reference and counter electrodes were glassy carbon, Ag/AgCl and Pt wire, respectively.

conditions at an electrode surface.[6, 45] Conversely, polycoltanates have not convincingly exhibited electroactivity in either aqueous or nonaqueous media on account of the considerable energy barrier towards reduction posed by their high standard reduction potentials and high negative charge densities. Substitution of metal centres in the polytungstate framework by other metals has a significant effect in the electrochemical properties of the resulting clusters, a phenomenon observed in theoretical[46] and experimental studies.[47]

Moreover, mixed Nb/W[18, 48] and Ta/W[15] polyanions show an equivalent electrochemical response to polytungstates inasmuch as the Nb/Ta ratio to W in the cluster remains sufficiently low. Therefore, we decided to investigate the electronic absorption and redox properties of **{Ta$_3$W$_3$}**, **{NbW$_9$}**, **{TaW$_9$}** and **{Ta$_2$W$_8$}** in aqueous solution by means of cyclic voltammetry (CV) and UV-visible spectroscopy (UV-vis).

The UV-vis spectra of **{NbW$_9$}**, **{TaW$_9$}** and **{Ta$_2$W$_8$}** are analogous and different to the spectrum of **{Ta$_3$W$_3$}** (Fig S17). The typical polyoxometalate UV band at 260 nm is present in the spectra of the four compounds. The spectra of **{NbW$_9$}**, **{TaW$_9$}** and **{Ta$_2$W$_8$}** show an additional band at different wavelengths around 300 nm (Fig 5) which is ascribed to the O→M charge transfer across the linear M-O$_d$-M bonds between the metal centres in the equatorial positions and the corresponding oxo ligands.[39] Interestingly, this band shows a hypsochromic (blue) shift as a function of the number of Nb or Ta centres present in the equatorial positions of the polyanion structure. The spectrum of $[W_{10}O_{32}]^{4-}$ shows this band at 322 nm, while the equivalent band in the spectra of **{NbW$_9$}**, **{TaW$_9$}** and **{Ta$_2$W$_8$}** is located at 309, 305 and 298 nm respectively. Substitution of decatungstate by a Re^V centre also results in a similar shift of that band in $[ReW_9O_{32}]^{5-}$.[40]

CV reveals a different electrochemical activity of polysubstituted **{Ta$_3$W$_3$}** and **{Ta$_2$W$_8$}**, compared to the monosubstituted clusters, **{NbW$_9$}** and **{TaW$_9$}**. The voltammograms of **{Ta$_3$W$_3$}** (Fig S18) and **{Ta$_2$W$_8$}** (Fig 6) show no redox waves in the potential window defined by the solvent. On the other hand, the voltammograms of both **{NbW$_9$}** and **{TaW$_9$}** display one irreversible redox process (Fig 6) at cathodic peak potentials of -562 and -539 mV, respectively. Interestingly, $[ReW_9O_{32}]^{5-}$ displays a similar electrochemical behaviour together with extensive decomposition during bulk electrolysis at potentials more cathodic than the first observed reduction wave.[40] The voltammogram of decatungstate was also recorded under the same conditions and the number and reversibility of redox couples is higher than in the substituted clusters. $\{W_{10}\}$ shows the typical one-electron reversible waves at $E_{1/2}$ of -112 and 353 mV followed by a two-electron quasi-reversible wave at -651 mV, values similar to the reported ones.[49] This pronounced difference in the electrochemical behaviour of substituted decatungstates and $\{W_{10}\}$ is presumably caused by two interrelated factors: 1) the substitution of W^{VI} centres by the less electrophilic Nb^V/Ta^V, which results in an increase of both the HOMO-LUMO energy gap (E_{gap}) (see below), and 2) the charge density of the cluster. This effect leads to a lower electron affinity, and to the subsequent cathodic shift, or complete disappearance, of the first reduction process in the substituted polytungstates.

Computational Characterization

We studied the electronic structure and properties of $\{W_{10}\}$, **{NbW$_9$}**, **{TaW$_9$}**, **{Ta$_2$W$_8$}**, and their reduced derivatives using first principles calculations. $\{W_{10}\}$ presents the characteristic POM electronic structure with the oxo and metal bands composed of the occupied O p- and empty W d-orbitals, respectively. The incorporation of Nb (**{NbW$_9$}**) and Ta (**{TaW$_9$}**) in the decatungstate framework does not result in significant changes in the electronic structure of the clusters; however, the frontier orbitals in the metal band only have a small contribution from the heterometal d-orbitals. This is attributed to the energy mismatch between the Nb/Ta and the W d orbitals which disfavours their mixing in the metal band.

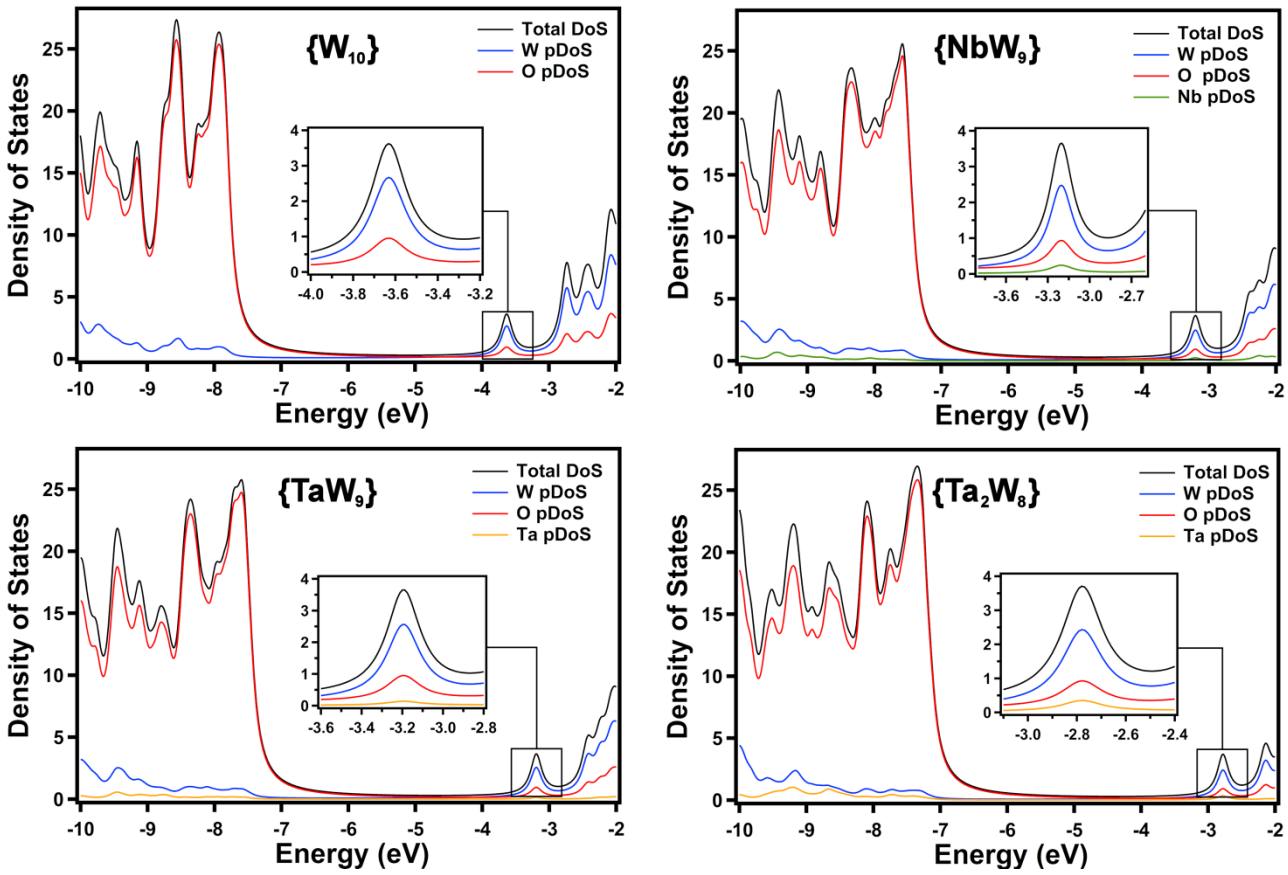

Fig 7. Density of States (DoS) of $\{W_{10}\}$ (top left), **{NbW$_9$}** (top right), **{TaW$_9$}** (bottom left) and **{Ta$_2$W$_8$}** (bottom right).

Identifying substitution position of the Nb/Ta in the tungstate clusters is challenged by the crystallographic disorder of these highly symmetric species; so we utilized computational methods, which confirmed our initial suppositions. Calculations of the relative energies of the two isomers of $\{MW_9\}$ (M = Nb, Ta) (Fig S32 and Table S43) indicate that Nb/Ta substitution is favoured at the equatorial position and disfavoured at the apical positions.

Analogous calculations conducted on the eight isomers of $\{M_2W_8\}$ (Fig S33 and Table S44) show that substitution at both apical positions is strongly disfavoured while substitution at equatorial positions is most preferred. Moreover, isomers disubstituted exclusively at equatorial positions and absent of a 180^o M-O-M bridge (M = Nb, Ta) are the most energetically stable. These results are in agreement with the experimental SXRD data which unambiguously confirm the location of the Nb centre at the equatorial positions in **{NbW$_9$}**.

The one-electron reduction of these species is localized at the equatorial W centres (M2, Fig S7) as the unpaired electron is delocalized across those centres. This is clearly indicated by the values of spin density, 0.118, 0.125 and 0.130 per W for $\{W_{10}\}$, **{NbW$_9$}** and **{TaW$_9$}** respectively, at the equatorial W positions. Furthermore, the spin density on the heterometals and on the apical W centres is negligible. In summary, the monoreduction of these polyanions leads to the formation of W^{VI}/W^{V} mixed valence species in which the W^{V} centre is delocalized among the equatorial sites of the cluster. This is in agreement with the Density of States (DoS) shown in Fig 7 where the valence band located in the -3 to -4 eV region is mainly composed of W d-orbitals. Our calculations on $\{W_{10}\}$ and its reduced derivatives are in perfect agreement studies.[46, 50] The calculated potentials for these one-electron reduction processes are also in agreement with the recorded potentials from CV experiments (Table 1). The presence of Ta^{V} or Nb^{V} in the cluster framework decreases the redox potential by *ca.* 0.35 V and this decrease is correlated with the higher LUMO energy in these substituted polyanions. Finally, it is worth noting that our calculated HOMO-LUMO gaps are systematically overestimated by *ca.* 0.26 eV with respect to those inferred by the UV-Vis spectra (Fig 4) as shown in Table 2; however, the gap is well-known to be highly dependent on the exchange-correlation functional and increase with the amount of Hartree-Fock exchange incorporated in hybrid functionals.[50]

Table 1. Experimental and calculated (B3LYP) redox potentials for $\{W_{10}\}$, **{NbW$_9$}** and **{TaW$_9$}** different species (vs Ag/AgCl). LUMO energy is also presented as it is correlated with the redox potential.

Reduction	Calculated (B3LYP)		Experimental
	LUMO (eV)	1st Red. Pot. (V)	1st Red. Pot. (V)
$[W_{10}O_{32}]^{4-} + 1e^- \rightarrow [W_{10}O_{32}]^{5-}$	-3.63	-0.14	-0.15
$[TaW_9O_{32}]^{5-} + 1e^- \rightarrow [TaW_9O_{32}]^{6-}$	-3.20	-0.55	-0.54
$[NbW_9O_{32}]^{5-} + 1e^- \rightarrow [NbW_9O_{32}]^{6-}$	-3.20	-0.54	-0.56

Table 2. Experimental and calculated (B3LYP) energy gaps (E_{gap}) for $\{W_{10}\}$, **{NbW$_9$}**, **{TaW$_9$}** and **{Ta$_2$W$_8$}**.

Cluster	Calc. (B3LYP) E_{gap} (eV)	Exp. E_{gap} (eV)[a]
$\{W_{10}\}$	4.18	3.85
{NbW$_9$}	4.25	4.01
{TaW$_9$}	4.27	4.07
{Ta$_2$W$_8$}	4.38	4.16

[a] Calculated as E=hc/λ, where λ is value of wavelength for the absorption ascribed to the O→M charge transfer across linear M-O-M bonds.

Conclusions

Here we have established the first W/Ta series of POMs and delineated the chemical behaviour as a function of W:Ta ratio. It is now firmly established that Ta can be incorporated into polytungstate clusters in acidic water. However, the relative instability of Ta-POMs shown here and elsewhere is consistent with the slow expansion of Ta-POM chemistry, in comparison to its group V/VI neighbours. For example, fragmentation of more Ta-rich clusters **{Ta$_3$W$_3$}** and **{Ta$_2$W$_8$}** in the gas phase is notably more extensive than that of **{TaW$_9$}**. There is growing evidence that protonation of Ta oxoanions and polyoxoanions at any pH is inherently less stable than protonation of the analogous Nb species. That is, protonated tantalate anions tend to polymerize and precipitate hydrous oxides, rather than reassemble and grow into higher nuclearity assemblies. These results open new avenues to control the self-assembly of mixed metal isopolyanions in solution and describe how the extent of the substitution affects the stability and electronic properties of the clusters. In addition, establishing systematic syntheses of these mixed-metal group V/VI clusters with varying ratio provide an excellent opportunity to expand our knowledge of the ion association of polyanions and cations in solution.[31, 32] The results of our ongoing investigations on this topic will be the subject of a future publication.

Acknowledgements

This work was supported by the U.S. Department of Energy, Office of Basic Energy Sciences, Divisions of Materials Sciences and Engineering, under award DE SC0010802. P.I.M. and M.N also wish to thank Karly Vial for her assistance in the synthesis of Cs**{Ta$_2$W$_8$}**, Dr. Eric Reinheimer for interesting discussions on the crystallographic analysis of Cs**{NbW$_9$}**, Cs**{TaW$_9$}** and Cs**{Ta$_2$W$_8$}** and Dr. Jun Li for her technical assistance in the thermogravimetric analysis of Cs**{TaW$_9$}**. P.M. thanks Prof. Thomas Heine for the scientific discussions and support on the computational characterization.

Notes and references

‡CCDC numbers (www.ccdc.cam.ac.uk): 1061587 (CsNa**{Ta$_3$W$_3$}**), 1061584 (Cs**{NbW$_9$}**), 1061586 (Cs**{TaW$_9$}**) and 1061585 (Cs**{Ta$_2$W$_8$}**).

†Synthesis of $Cs_4Na[Ta_3W_3O_{19}]\cdot 6H_2O$ (CsNa**{Ta$_3$W$_3$}**): $Cs_3[Ta(O_2)_4]$ (3.0 g, 4.2 mmol) was added to a solution of $Na_2WO_4\cdot 2H_2O$ (3.3 g, 10.0 mmol) 30 mL of H_2O. The pH of the resulting turbid solution was adjusted to 8.0 by the dropwise addition of HCl (37%, v/v). The thin suspension thus obtained was refluxed for 5 h and the resulting mixture was centrifuged at room temperature. Colourless crystals plates of CsNa**{Ta$_3$W$_3$}** formed overnight in the supernatant placed at 4 °C in a cold chamber. Yield (crystals): 0.783 g (25% based on Ta). Atomic ratios (EDX) calculated (found): W/Ta 1.0 (1.0), W/Cs 0.8 (0.7). Characteristic IR bands (cm^{-1}): 537 (sh), 572 (sh), 772 (sh), 887 (w), 934 (s). UV absorption: λ (O→M) = 256 nm, ε = 2.0 x 10^4 mol^{-1} L cm^{-1}. Water content (%), crystallographic (TGA crystals, 22-200 °C, in air): 5.2 (5.4). Crystallographic Data for CsNa**{Ta$_3$W$_3$}**: formula, $Cs_4H_{12}NaO_{25}Ta_3W_3$; MW = 2061.3 g mol^{-1}; size, (0.16 x 0.12 x 0.04) mm^3; T = 173 K; crystal system, trigonal; space group R-3; a = 9.3948(3) Å; b = 9.3948(3) Å; c = 28.2796(11) Å; V = 2161.62(16) Å^3; Z = 3; D_c = 4.750 Mg/m^3; μ = 28.348 mm^{-1}; F(000) = 2652; $2\vartheta_{max}$ = 74.29°; 14994 reflections; 2432 independent reflections [R_{int} = 0.0455]; $R1$ = 0.0342; w$R2$ = 0.0849 and GOF = 1.116 for 2432 reflections (57 parameters) with $I>2\sigma(I)$, $R1$ = 0.0423, w$R2$ = 0.0880 and GOF = 1.116 for all reflections; max/min residual electron density +3.436/-3.627 eÅ^3.

†Synthesis of $Cs_5[NbW_9O_{32}]\cdot 7.5H_2O$ (Cs**{NbW$_9$}**): $K_3[Nb(O_2)_4]$ (1.1 g, 3.3 mmol) was dissolved in 25 mL of H_2O at 70 °C. In a separate beaker, $Na_2WO_4\cdot 2H_2O$ (3.6 g, 11 mmol) was dissolved in a mixture of H_2O (11.9 mL) and H_2O_2 (0.65 mL, 30% v/v). The contents of the two beakers were then combined and stirred for 30 min at 70 °C to afford a clear solution. The pH of this solution was adjusted to 2.0 (3M H_2SO_4) and the resulting mixture was first refluxed for 2 h and then centrifuged at room temperature. CsCl (5.6 g, 33 mmol) was added to the supernatant under vigorous stirring and the thick yellow suspension thus obtained was stirred for *ca.* 3 min and filtrated under vacuum. The isolated yellow precipitate was finally washed with cold water (2 mL) and dried under suction. Yield (crude product) = 2.089 g (21%, Nb). Analytically pure crystals of Cs**{NbW$_9$}** were obtained by recrystallizing this crude product twice from the minimum amount of boiling water and these crystals were subsequently used for further characterization. Atomic ratios (EDX) calculated (found): W/Nb 9.0 (8.7), W/Cs 1.8 (1.8). Characteristic IR bands (cm^{-1}): 565 (s), 572 (s), 656 (s), 754 (vs), 879 (sh), 948 (vsh) 991 (vw). UV absorption: λ_1 (O→M, shoulder) = 260 nm, ε_1 = 13.2 x 10^4 mol^{-1} L cm^{-1}, λ_2 (O→M, band) = 309 nm, ε_2 = 10.1 x 10^4 mol^{-1} L cm^{-1}. Water content (%), crystallographic (TGA, 22-200 °C, in air): 4.1 (4.0). Crystallographic data for Cs**{NbW$_9$}**: $Cs_5H_{15}O_{39.50}NbW_9$, MW = 3059.9 g mol^{-1}; size, (0.14 x 0.13 x 0.09) mm^3; T = 193 K; crystal system, triclinic; space group, P-1; a = 9.8464(4) Å; b = 10.2634(4) Å; c = 11.5535(4) Å; α = 99.160(2)°; β = 100.815(2)°; γ = 115.949(2)°; V = 991.98(7) Å^3; Z = 1; D_c = 5.108 Mg/m^3; μ = 30.880 mm^{-1}; F(000) = 1306; $2\vartheta_{max}$ = 56.0°; 17629 reflections; 4770 independent reflections [R_{int} = 0.0643]; $R1$ = 0.0365; w$R2$ = 0.0690 and GOF = 1.021 for 4770 reflections (268

parameters) with $I>2\sigma(I)$; $R1$ = 0.0561; w$R2$ = 0.0760 and GOF = 1.021 for all reflections; max/min residual electron density +1.838/-1.809 eÅ^3.

† Synthesis of $Cs_5[TaW_9O_{32}]\cdot 6.5H_2O$ (Cs**{TaW$_9$}**): $K_3[Ta(O_2)_4]$ (2.0 g, 4.7 mmol) was added at room temperature to a stirred solution of $Na_2WO_4\cdot 2H_2O$ (6.6 g, 20.0 mmol) in 40 mL of hot (ca 60 ^oC) H_2O. The pH of the resulting mixture was carefully adjusted to 2.0 by the dropwise addition of HCl (37% w/w). The yellow suspension was refluxed for 2 h and centrifuged at room temperature. CsCl (10.0 g, 59.4 mmol) was added to the isolated bright yellow supernatant and a mass of light orange solids was isolated from the resulting suspension by centrifugation, washed twice with 5 mL of water, twice with 20 mL of 2-propanol and finally dried under vacuum. This crude product was dissolved in 30 mL of boiling H_2O and yellow crystal plates formed overnight at 4oC. Yield (crude product) = 2.55 g (17.3 %, Ta). Atomic ratios (EDX) calculated (found): W/Ta 9.0 (7.4), W/Cs 1.8 (1.9). Characteristic IR bands (cm^{-1}): 549 (s), 572 (s), 655 (s), 772 (vs), 885 (s), 953 (vs). UV absorption: λ_1 (O→M, shoulder) = 260 nm, ε_1 = 3.7 x 10^4 mol^{-1} L cm^{-1}, λ_2 (O→M, band) = 305 nm, ε_2 = 2.8 x 10^4 mol^{-1} L cm^{-1}. Water content (%), crystallographic (TGA, 22-200 ^oC, in air): 4.0 (4.5). Crystallographic data for Cs**{TaW$_9$}**: $Cs_5H_{13}O_{38.5}TaW_9$, MW = 3129.9 g mol^{-1}; size, (0.08 x 0.06 x 0.04) mm^3; T = 193 K, crystal system, triclinic; space group, *P*-1; a = 9.783(3) Å; b = 10.175(3) Å; c = 11.464(3) Å; α = 99.025(5)°; β = 100.999(5)°; γ = 115.804(6)°; V = 970.6(5) Å^3; Z = 1; D_c = 5.354 Mg/m^3; μ = 34.077 mm^{-1}; $F(000)$ = 1335; $2\vartheta_{max}$ = 56.0°; 16826 reflections; 4675 independent reflections [R_{int} = 0.0621], $R1$ = 0.0322; w$R2$ = 0.0698 and GOF = 1.036 for 4675 reflections (253 parameters) with $I>2\sigma(I)$, $R1$ = 0.0480, w$R2$ = 0.0756 and GOF = 1.036 for all reflections, max/min residual electron density +2.913/-1.928 eÅ^3.

†Synthesis of $Cs_6[Ta_2W_8O_{32}]\cdot 6H_2O$ (Cs**{Ta$_2$W$_8$}**): The synthetic procedure to prepare this compound was analogous to the one used for Cs**{TaW$_9$}** save for the amount of $Na_2WO_4\cdot 2H_2O$ (3.3 g, 10.0 mmol). Yield (crude product) = 0.165 g (1 %, Ta). Atomic ratios (EDX) calculated (found): W/Ta 4.0 (3.8), W/Cs 1.3 (1.5). Characteristic IR bands (cm^{-1}): 534 (s), 648(s), 769 (sh), 880 (s), 946 (vsh). UV absorption: λ_1 (O→M, shoulder) = 260 nm, ε_1 = 3.3 x 10^{-4} mol^{-1} L cm^{-1}, λ_2 (O→M, band) = 298 nm, ε_2 = 3.3 x 10^{-4} mol^{-1} L cm^{-1}. Water content (%), crystallographic (TGA, 26-200 ^oC, in air): 3.5 (3.5). Crystallographic Data for Cs**{Ta$_2$W$_8$}**: $Cs_6H_{12}O_{38}Ta_2W_8$; M = 3250.8 g mol^{-1}; size, (0.07 x 0.04 x 0.02) mm^3; T = 200(2) K; crystal system, triclinic; space group, *P*-1; a = 9.798(6) Å; b = 10.273(6) Å; c = 11.322(7) Å; α = 92.172(9)°; β = 101.597(9)°; γ = 115.836(7)°; V = 994.6(11) Å^3; Z = 1; D_c = 5.426 Mg/m^3; μ = 34.014 mm^{-1}; $F(000)$ = 1384; $2\vartheta_{max}$ = 56.0°, 12962 reflections; 4791 independent reflections [R_{int} = 0.0783]; $R1$ = 0.0502; w$R2$ = 0.0912 and GOF = 1.025 for 4791 reflections (241 parameters) with $I>2\sigma(I)$, $R1$ = 0.0938, w$R2$ = 0.1087 and GOF = 1.025 for all reflections, max/min residual electron density +5.545/-2.705 eÅ^3.

1 M. T. Pope, *Heteropoly and Isopolyoxometalates*, Springer-Verlag, Berlin, 1983.
2 M. Nyman, *Dalton Trans.*, 2011, **40**, 8049-8058.
3 This term is derived from "coltan", an abbreviation for columbite-tantalite, the ore from which Nb and Ta are extracted (D. A. R. Mackay and G. J. Simandl; *Miner Deposita*, 2014, **49**, 1025-1047).
4 M. Nyman, T. M. Alam, F. Bonhomme, M. A. Rodriguez, C. S. Frazer and M. E. Welk, *J. Cluster Sci.*, 2006, **17**, 197-219.
5 Y. Hou, M. Nyman and M. A. Rodriguez, *Angew. Chem. Int. Edit*, 2011, **50**, 12514-12517.
6 M. Sadakane and E. Steckhan, *Chem. Rev.*, 1998, **98**, 219-237.
7 C. L. Hill and C. M. Prosser-McCartha, *Coord. Chem. Rev.*, 1995, **143**, 407-455.
8 I. V. Kozhevnikov, *Chem. Rev.* , 1998, **98**, 171-198.
9 A. Bashan and A. Yonath, *J. Mol. Struct.*, 2008, **890**, 289-294.
10 H. N. Miras, L. Vila-Nadal and L. Cronin, *Chem. Soc. Rev.*, 2014, **43**, 5679-5699.
11 D. Zhang, C. Zhang, P. Ma, B. S. Bassil, R. Al-Oweini, U. Kortz, J. Wang and J. Niu, *Inorg. Chem. Front.*, 2015, **2**, 254-262.
12 D. Zhang, Z. Liang, S. Xie, P. Ma, C. Zhang, J. Wang and J. Niu, *Inorg. Chem.*, 2014, **53**, 9917-9922.
13 D. J. Edlund, R. J. Saxton, D. K. Lyon and R. G. Finke, *Organometallics*, 1988, **7**, 1692-1704.
14 R. G. Finke and M. W. Droege, *J. Am. Chem. Soc.*, 1984, **106**, 7274-7277.
15 S. Li, S. Liu, S. Liu, Y. Liu, Q. Tang, Z. Shi, S. Ouyang and J. Ye, *J. Am. Chem. Soc.*, 2012, **134**, 19716-19721.
16 S.-Q. Shi, Y.-G. Chen, J. Gong, Z.-M. Dai and L.-Y. Qu, *Transition Met. Chem.* , 2005, **30**, 136-140.
17 M. Dabbabi and M. Boyer, *J. Inorg. Nucl. Chem.*, 1976, **38**, 1011-1014.
18 M. Dabbabi, M. Boyer, J. P. Launay and Y. Jeannin, *J. Electroanal. Chem. Interfacial Electrochem.*, 1977, **76**, 153-164.
19 K. Bouadjadja-Rohan, C. Lancelot, M. Fournier, A. Bonduelle-Skrzypczak, A. Hugon, O. Mentre and C. Lamonier, *Eur. J. Inorg. Chem.*, 2015, DOI: 10.1002/ejic.201403160, 2067-2075.
20 F. Bannani, H. Driss, R. Thouvenot and M. Debbabi, *J. Chem. Crystallogr.*, 2007, **37**, 37-48.
21 M. C. Kaezer França, J.-G. Eon, M. Fournier, E. Payen and O. Mentre, *Solid State Sci.*, 2005, **7**, 1533-1541.
22 V. W. Day, W. G. Klemperer and C. Schwartz, *J. Am. Chem. Soc.*, 1987, **109**, 6030-6044.
23 C. J. Besecker, W. G. Klemperer, D. J. Maltbie and D. A. Wright, *Inorg. Chem.*, 1985, **24**, 1027-1032.
24 C. Sanchez, J. Livage, J. P. Launay and M. Fournier, *J. Am. Chem. Soc.*, 1983, **105**, 6817-6823.
25 H. Driss, K. Boubekeur, M. Debbabi and R. Thouvenot, *Eur. J. Inorg. Chem.*, 2008, DOI: 10.1002/ejic.200800235, 3678-3686.
26 F. Bannani, R. Thouvenot and M. Debbabi, *Eur. J. Inorg. Chem.*, 2007, DOI: 10.1002/ejic.200700357, 4357-4363.
27 C. J. Besecker, V. W. Day, W. G. Klemperer and M. R. Thompson, *J. Am. Chem. Soc.*, 1984, **106**, 4125-4136.
28 Y.-J. Lu, R. Lalancette and R. H. Beer, *Inorg. Chem.*, 1996, **35**, 2524-2529.
29 F. Bannani, H. Driss, M. Debbabi and R. Thouvenot, *J. Soc. Chim. Tunis.*, 2011, **13**, 85-91.
30 T. M. Anderson, M. A. Rodriguez, F. Bonhomme, J. N. Bixler, T. M. Alam and M. Nyman, *Dalton Trans.*, 2007, DOI: 10.1039/b707636c, 4517-4522.
31 M. R. Antonio, M. Nyman and T. M. Anderson, *Angew. Chem. Int. Ed.*, 2009, **48**, 6136-6140.
32 L. B. Fullmer, P. I. Molina, M. R. Antonio and M. Nyman, *Dalton Trans.*, 2014, **43**, 15295-15299.
33 D. Bayot and M. Devillers, *Coord. Chem. Rev.*, 2006, **250**, 2610-2626.
34 H. Hartl, F. Pickhard, F. Emmerling and C. Roehr, *Z. Anorg. Allg. Chem.*, 2001, **627**, 2630-2638.
35 J. A. Santos, Proceedings of the Royal Society of London. Series A, Mathematical and Physical Sciences, 1935, **150**, 309-322.
36 F. Pickhard and H. Hartl, *Z. Anorg. Allg. Chem.*, 1997, **623**, 1311-1316.
37 K. H. Tytko, J. Mehmke and S. Fischer, *Struct. Bonding* 1999, **93**, 129-321.
38 C. Rocchiccioli-Deltcheff, R. Thouvenot and M. Dabbabi, *Spectrochim. Acta, Part A*, 1977, **33A**, 143-153.
39 S. C. Termes and M. T. Pope, *Inorg. Chem.*, 1978, **17**, 500-501.

40 F. Ortega, M. T. Pope and H. T. Evans, Jr., *Inorg. Chem.*, 1997, **36**, 2166-2169.
41 A. J. Bridgeman and G. Cavigliasso, *J. Phys. Chem. A*, 2002, **106**, 6114-6120.
42 L. Vila-Nadal, A. Rodriguez-Fortea, L.-K. Yan, E. F. Wilson, L. Cronin and J. M. Poblet, *Angew. Chem., Int. Ed.*, 2009, **48**, 5452-5456.
43 F. Sahureka, R. C. Burns and E. I. von Nagy-Felsobuki, *Inorg. Chim. Acta*, 2003, **351**, 69-78.
44 R. J. Errington, G. Harle, W. Clegg and R. W. Harrington, *Eur. J. Inorg. Chem.*, 2009, DOI: 10.1002/ejic.200900640, 5240-5246.
45 M. S. Balula, J. A. Gamelas, H. M. Carapuca, A. M. V. Cavaleiro and W. Schlindwein, *Eur. J. Inorg. Chem.*, 2004, DOI: 10.1002/ejic.200300292, 619-628.
46 X. Lopez, J. J. Carbo, C. Bo and J. M. Poblet, *Chem. Soc. Rev.*, 2012, **41**, 7537-7571.
47 L. Parent, P. A. Aparicio, P. de Oliveira, A.-L. Teillout, J. M. Poblet, X. Lopez and I. M. Mbomekalle, *Inorg. Chem.*, 2014, **53**, 5941-5949.
48 Y. Ren, Y. Hu, Y. Shan, Z. Kong, M. Gu, B. Yue and H. He, *Inorg. Chem. Commun.*, 2014, **40**, 108-111.
49 A. Chemseddine, C. Sanchez, J. Livage, J. P. Launay and M. Fournier, *Inorg. Chem.*, 1984, **23**, 2609-2613.
50 D. Ravelli, D. Dondi, M. Fagnoni, A. Albini and A. Bagno, *Phys. Chem. Chem. Phys.*, 2013, **15**, 2890-2896.

Table of Contents (graphical abstract)

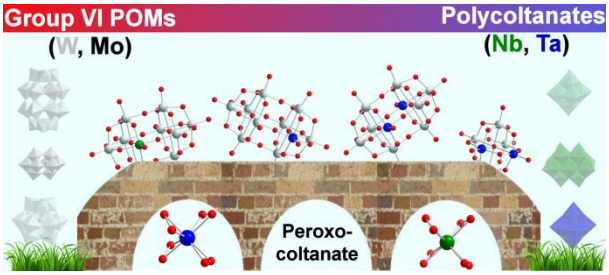

Reaction of Ta peroxometalate and tungstate affords the first systematic series of Ta/W isopolyoxometalates. An analogous reaction system yields a Nb/W cluster. The electronic structure and stability of these clusters varies as a function of the group V metal content, as inferred from spectroscopic, electrochemical and mass-spectrometry analysis and confirmed by DFT calculations.